Role of iodine recycling on sea-salt aerosols in the global marine boundary layer

Qinyi Li[1], Yee Jun Tham[2,3], Rafael P. Fernandez[4,5], Xu-Cheng He[3], Carlos A. Cuevas[1], and Alfonso Saiz-Lopez[1,*]

[1] Department of Atmospheric Chemistry and Climate, Institute of Physical Chemistry Rocasolano, CSIC, Madrid 28006, Spain;
[2] School of Marine Sciences, Sun Yat-Sen University, Zhuhai 519082, China;
[3] Institute for Atmospheric and Earth System Research / Physics, Faculty of Science, University of Helsinki, Helsinki 00014, Finland.
[4] Institute for Interdisciplinary Science, National Research Council (ICB-CONICET), Mendoza, 5501, Argentina
[5] School of Natural Sciences, National University of Cuyo (FCEN-UNCuyo), Mendoza, 5501, Argentina

[*] Corresponding author: Alfonso Saiz-Lopez (a.saiz@csic.es)

Contents of this file

Table S1. CAM-Chem simulation design

Case	HOI uptake coefficient	IBr yield	ICl yield
Base	0.06	0.0	0.0
Conventional	0.06	0.5	0.5
Updated	0.3	0.5	0.5
Upper-limit	0.9	0.5	0.5

20 **Table S2.** Comparison of simulated and observed O_3 at coastal sites around the globe from TOAR database (Archibald et al., 2020)

No.	lat	lon	Observation [a]	Base			Conventional			Updated			Upper-limit		
				Mean [b]	MB [c]	NMB [d]	Mean	MB	NMB	Mean	MB	NMB	Mean	MB	NMB
S1	63.7	-149.0	33.1	33.9	0.8	0.02	33.4	0.2	0.01	32.7	-0.5	-0.01	31.4	-1.7	-0.05
S2	54.9	8.3	33.3	31.7	-1.6	-0.05	31.3	-1.9	-0.06	30.9	-2.4	-0.07	30.1	-3.1	-0.09
S3	54.3	8.6	30.9	29.6	-1.2	-0.04	29.3	-1.6	-0.05	28.9	-2.0	-0.06	28.1	-2.7	-0.09
S4	54.3	13.3	30.3	32.2	1.9	0.06	31.9	1.6	0.05	31.5	1.2	0.04	30.8	0.5	0.02
S5	53.7	7.2	30.9	29.9	-1.0	-0.03	29.6	-1.3	-0.04	29.2	-1.7	-0.06	28.4	-2.5	-0.08
S6	53.6	8.1	28.0	29.9	1.9	0.07	29.6	1.6	0.06	29.2	1.2	0.04	28.4	0.4	0.01
S7	53.4	7.2	28.2	29.9	1.7	0.06	29.6	1.4	0.05	29.2	0.9	0.03	28.4	0.2	0.01
S8	44.4	-68.3	35.1	35.1	0.0	0.00	34.8	-0.4	-0.01	34.3	-0.8	-0.02	34.0	-1.2	-0.03
S9	40.3	-74.9	29.4	32.1	2.7	0.09	31.8	2.4	0.08	31.4	2.0	0.07	30.7	1.3	0.04
S10	36.5	-121.2	30.7	36.1	5.3	0.17	35.3	4.5	0.15	34.4	3.7	0.12	33.2	2.4	0.08
S11	34.9	-76.6	33.8	36.3	2.5	0.07	35.7	1.9	0.06	35.2	1.4	0.04	35.8	2.0	0.06
S12	30.7	-94.7	24.9	33.5	8.6	0.35	33.0	8.1	0.33	32.6	7.7	0.31	31.9	7.1	0.28
S13	30.1	-85.0	24.8	34.9	10.1	0.41	34.2	9.4	0.38	33.7	8.9	0.36	32.9	8.1	0.33
S14	27.8	-80.5	33.6	37.3	3.7	0.11	36.6	3.0	0.09	36.0	2.4	0.07	34.9	1.3	0.04
S15	24.3	154.0	27.2	26.6	-0.6	-0.02	25.5	-1.6	-0.06	24.6	-2.5	-0.09	22.4	-4.8	-0.18
S16	19.5	-155.6	35.9	26.1	-9.8	-0.27	24.5	-11.4	-0.32	23.0	-12.9	-0.36	20.1	-15.8	-0.44
S17	-33.7	-71.0	13.8	28.6	14.7	1.06	28.0	14.1	1.02	27.5	13.6	0.98	26.7	12.9	0.93

[a] annual average of observed O_3 in nmol mol^{-1} (ppbv).
[b] annual average of simulated O_3 in ppbv.
[c] mean bias in ppbv.
[d] normalized mean bias.

Table S3. Evaluation of CAM-Chem IO simulation

Location (Reference)	Period	Observation [a]	BASE [b]	Conventional [b]	Updated [b]	Upper-limit [b]
Cape Verde (Read et al., 2008; Mahajan et al., 2010)	Nov 2006 to Jun 2007	1.0 to 1.7	0.31 (0.15 to 0.67)	0.48 (0.29 to 1.06)	0.53 (0.31 to 1.15)	0.58 (0.36 to 1.20)
Western Pacific (Großmann et al., 2013)	Oct 2009	0.7 to 1.4	0.73 (0.46 to 0.73)	0.86 (0.57 to 0.86)	0.92 (0.63 to 0.92)	0.98 (0.67 to 0.98)
Central Pacific (Dix et al.2013)	Jan 2010	0.5 to 0.6	0.41 (0.19 to 0.56)	0.60 (0.38 to 0.78)	0.70 (0.45 to 0.88)	0.77 (0.48 to 0.89)
Eastern Pacific (Mahajan et al., 2012)	Apr 2010	0.3 to 0.9	0.72 (0.47 to 0.72)	0.94 (0.60 to 0.94)	1.00 (0.65 to 1.00)	1.04 (0.71 to 1.04)
Southern Atlantic (Prados-Roman et al., 2015)	Jan 2011 to Feb 2011	0.3 to 0.6	0.27 (0.25 to 0.43)	0.43 (0.41 to 0.58)	0.46 (0.44 to 0.64)	0.47 (0.45 to 0.67)
Southern Indian Ocean (Prados-Roman et al., 2015)	Feb 2011 to Mar 2011	0.4 to 0.8	0.28 (0.23 to 0.57)	0.49 (0.43 to 0.69)	0.53 (0.47 to 0.75)	0.54 (0.47 to 0.80)
Southern Pacific (Prados-Roman et al., 2015)	Apr 2011 to May 2011	0.3 to 0.7	0.26 (0.15 to 0.26)	0.36 (0.26 to 0.52)	0.40 (0.27 to 0.55)	0.43 (0.28 to 0.55)
Northeastern Pacific (Prados-Roman et al., 2015)	May 2011 to Jun 2011	0.3 to 0.8	0.55 (0.38 to 0.60)	0.74 (0.50 to 0.80)	0.82 (0.56 to 0.88)	0.88 (0.62 to 0.93)
Northern Atlantic (Prados-Roman et al., 2015)	Jun 2011 to July 2011	0.4 to 0.8	0.60 (0.36 to 0.89)	0.74 (0.47 to 1.04)	0.77 (0.51 to 1.08)	0.83 (0.56 to 1.14)
Galápagos Islands (Gómez Martín et al., 2013)	Sep 2010 to Feb 2012	0.4 to 0.5	0.59 (0.36 to 1.03)	0.82 (0.59 to 1.39)	0.94 (0.71 to 1.56)	1.05 (0.79 to 1.72)
Indian Ocean (Mahajan et al., 2019a)	Jan-Feb 2015	0.1 to 1.7	0.61 (0.29 to 0.81)	0.78 (0.43 to 0.95)	0.83 (0.50 to 1.00)	0.87 (0.54 to 1.04)
Northern and Equatorial Indian Ocean (Mahajan et al., 2019b)	Dec 2015	0.1 to 0.5	1.22 (0.27 to 1.61)	1.42 (0.43 to 1.75)	1.49 (0.51 to 1.79)	1.55 (0.56 to 1.85)
Eastern Pacific (Dix et al., 2016)	Jan to Feb 2012	0.1 to 0.8	0.38 (0.33 to 0.56)	0.54 (0.48 to 0.72)	0.59 (0.53 to 0.78)	0.62 (0.56 to 0.82)
Western Pacific, Tropics (Takashima et al., 2021)	Nov to Dec 2014	0.3 to 0.8	0.67 (0.39 to 0.87)	0.83 (0.51 to 1.02)	0.90 (0.56 to 1.08)	0.94 (0.60 to 1.13)

[a] Observation results are in pmol/mol (pptv) and are daytime average in MBL.
[b] Simulation results for year 2018 are stated in the same unit (pptv) and level (lower than 1000m) as observation data. Simulations are presented as monthly sunlit time average ranges (in the same months as measurement and the range of monthly average in year 2018 in the parentheses. Simulations are averaged in a rectangular area covering the tracks of ships or flights.

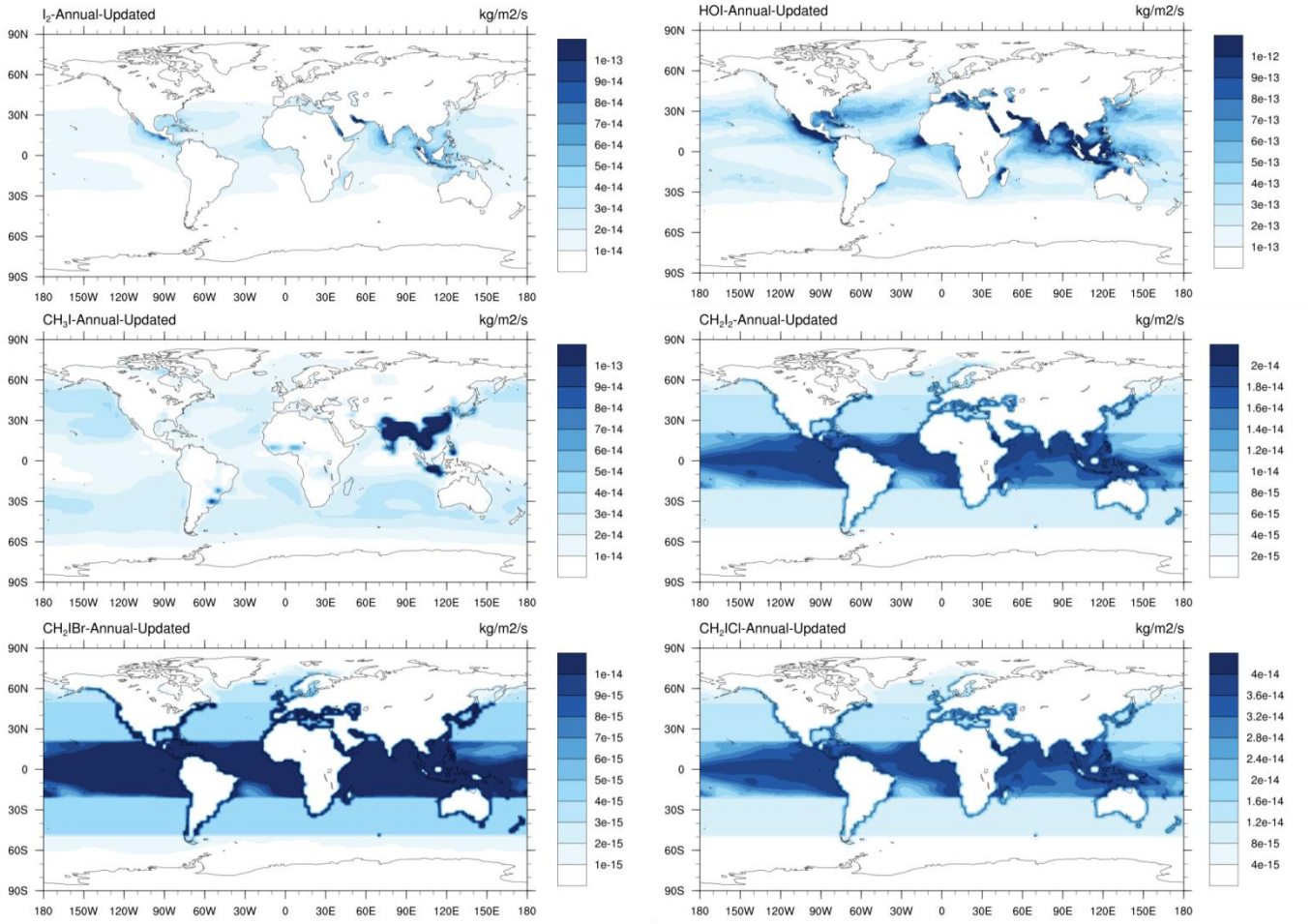

Figure S1. Annual mean Inorganic and organic iodine species emission fluxes (kg/m^2/s).

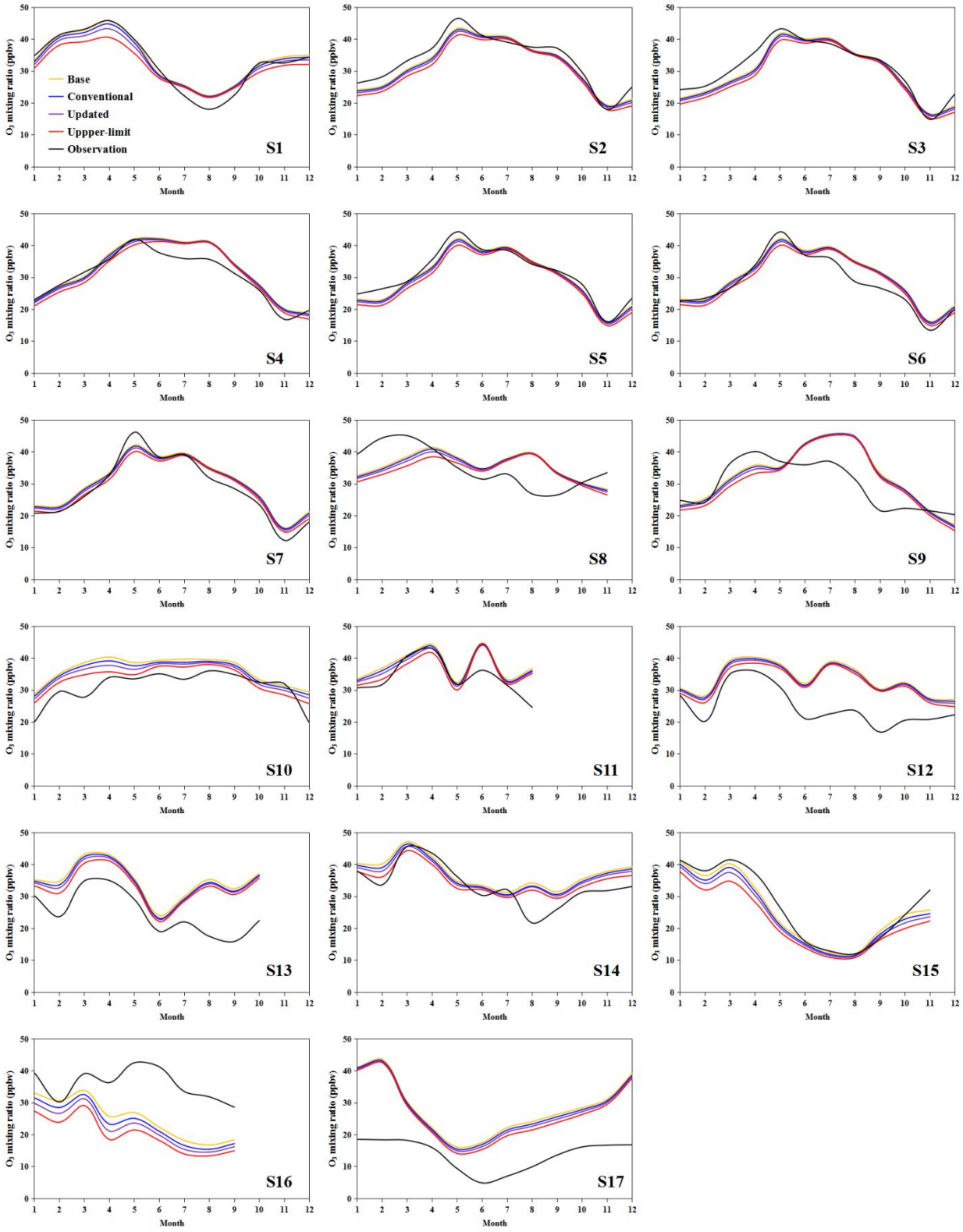

Figure S2. Comparison of observed and **s**imulated monthly variation of O_3 at coastal sites. The locations of these sites are shown in Table S2.

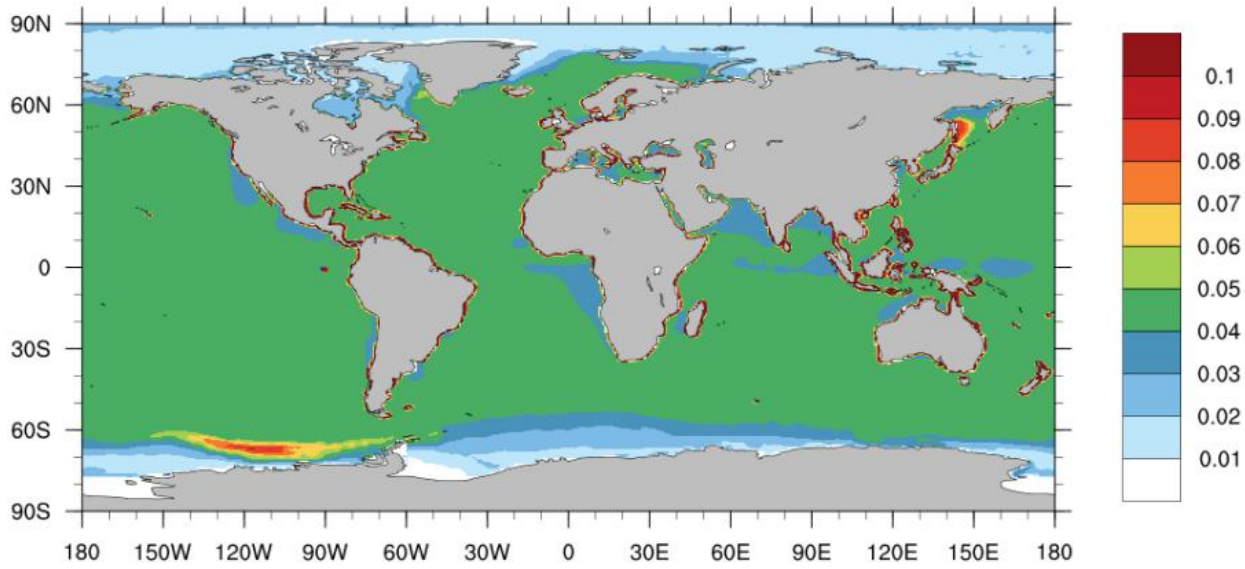

Figure S3. Simulated distribution of the annual mean O_3 deposition velocity (cm/s) over the ocean in the Updated case, with a global average of 0.046 cm/s. Note that the difference of O_3 deposition velocity among the BASE, Conventional, Updated, and Upper-limit cases is negligible (<1%).

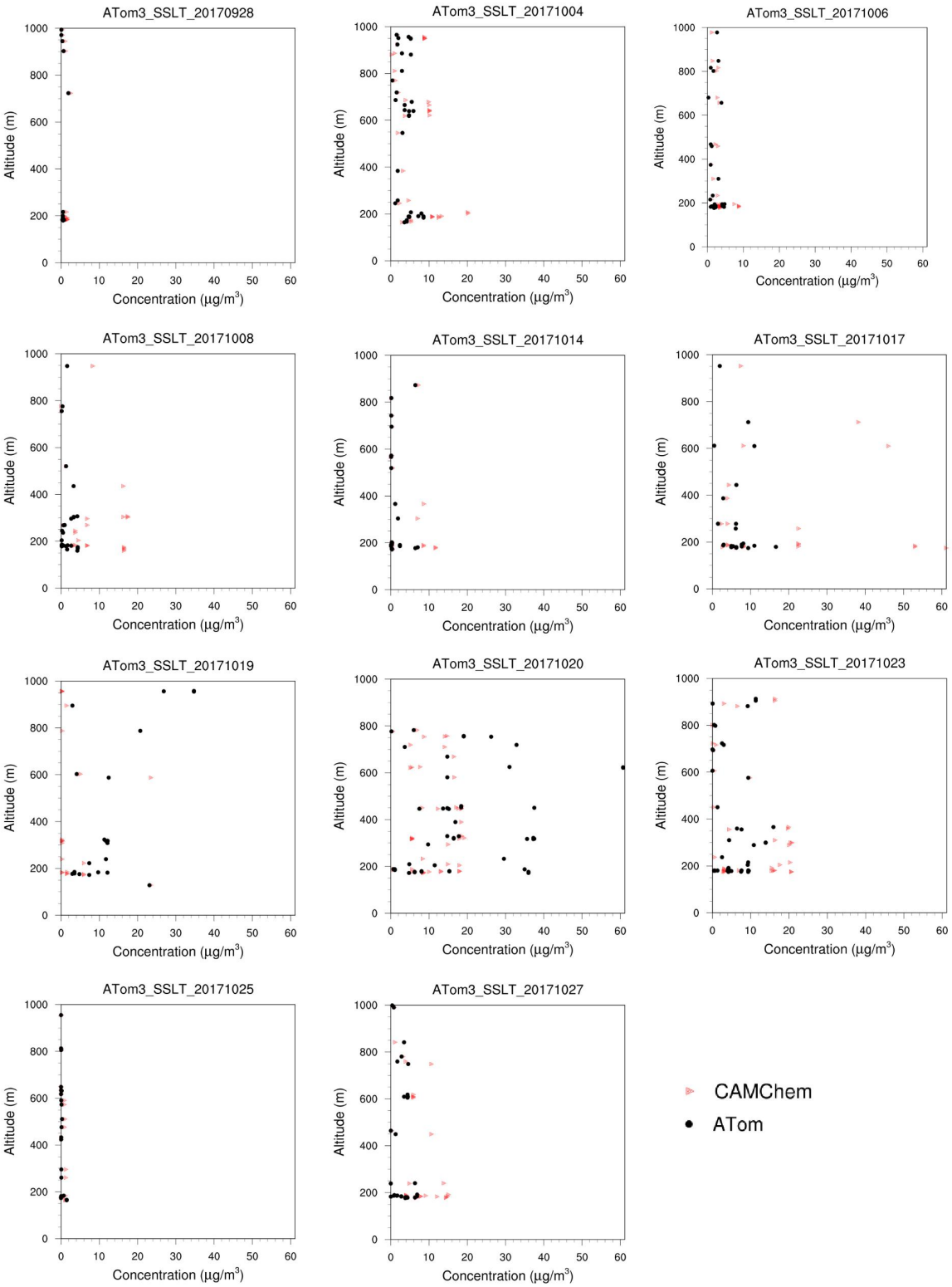

Figure S4. Comparison of observed and simulated sea-salt aerosol concentration (µg m^{-3}). The observed SSA concentrations are obtained from the ATom campaign (https://doi.org/10.3334/ORNLDAAC/1581; ATom3: Sep to Oct, 2017; ATom4: Apr to May, 2018). The simulated SSA concentrations are CAM-Chem output at the same location and altitude as the corresponding observations. The simulated SSA levels are consistent with the observations during most flights within the marine boundary layer (<1000m above sea level).

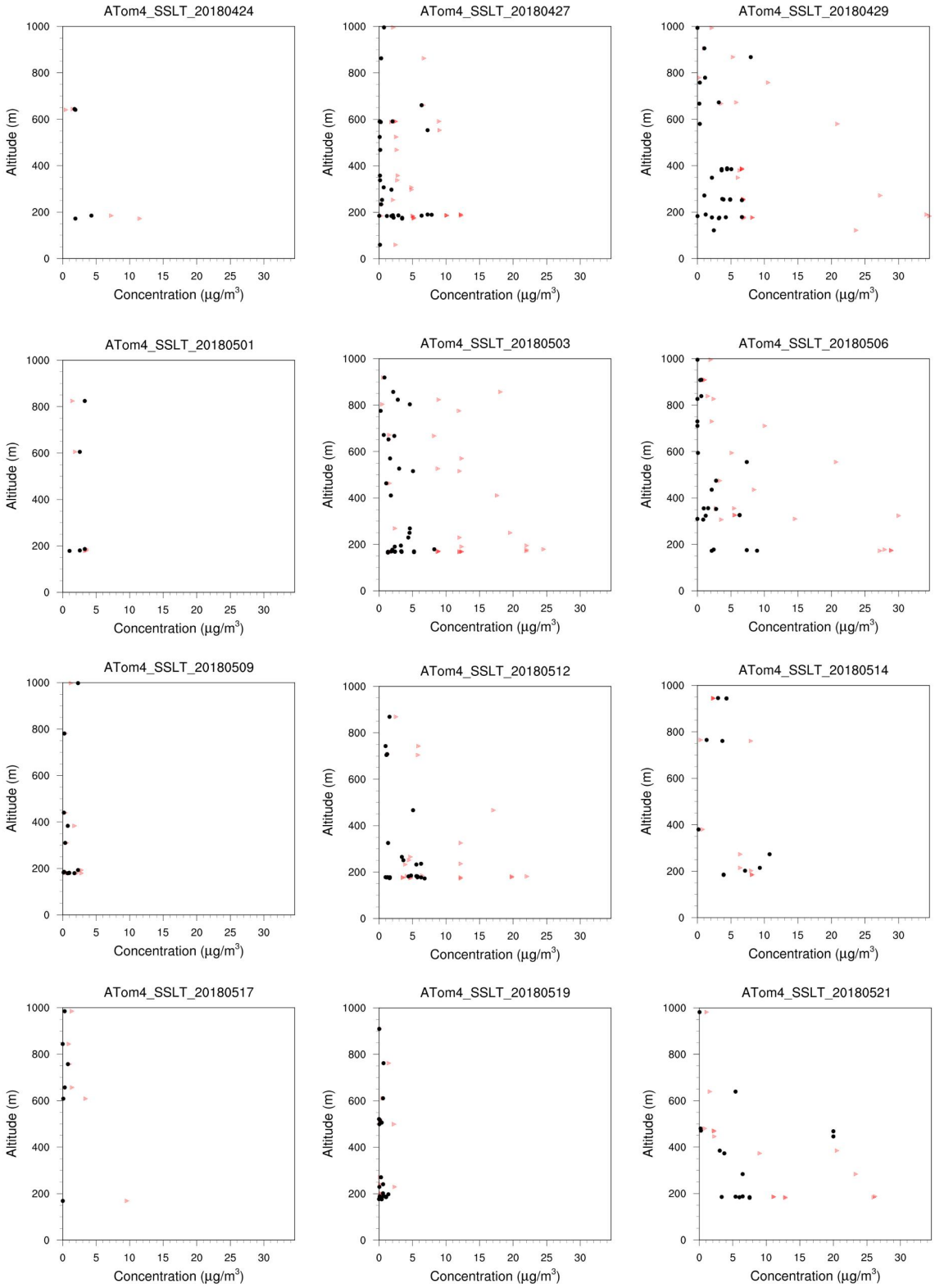

(Continued) **Figure S4**.

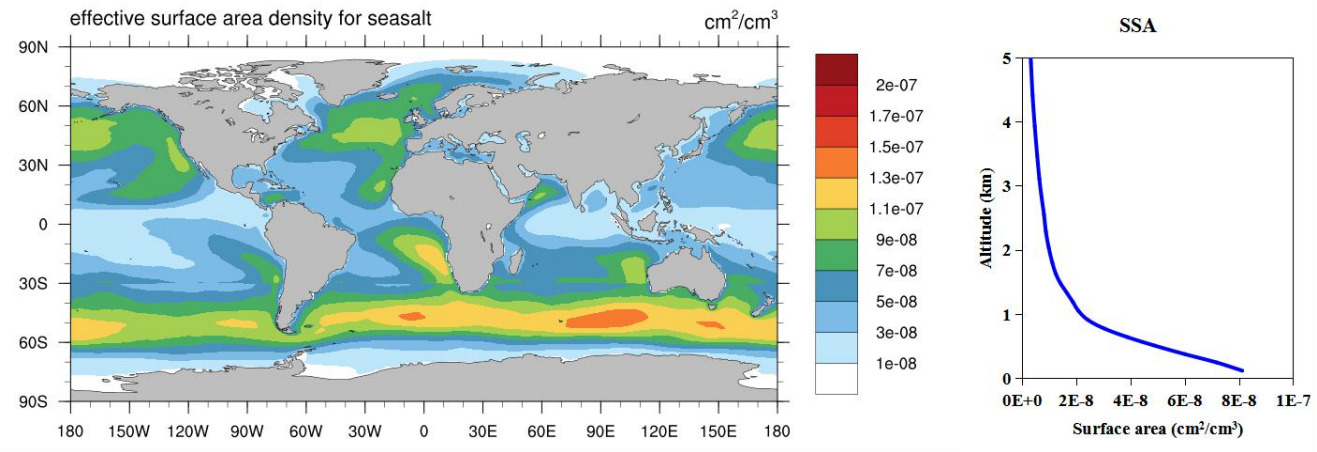

Figure S5. Simulated distribution of the annual mean surface area of sea-salt aerosol (cm^2/cm^3) averaged in the MBL (left) and in the vertical profile (right).

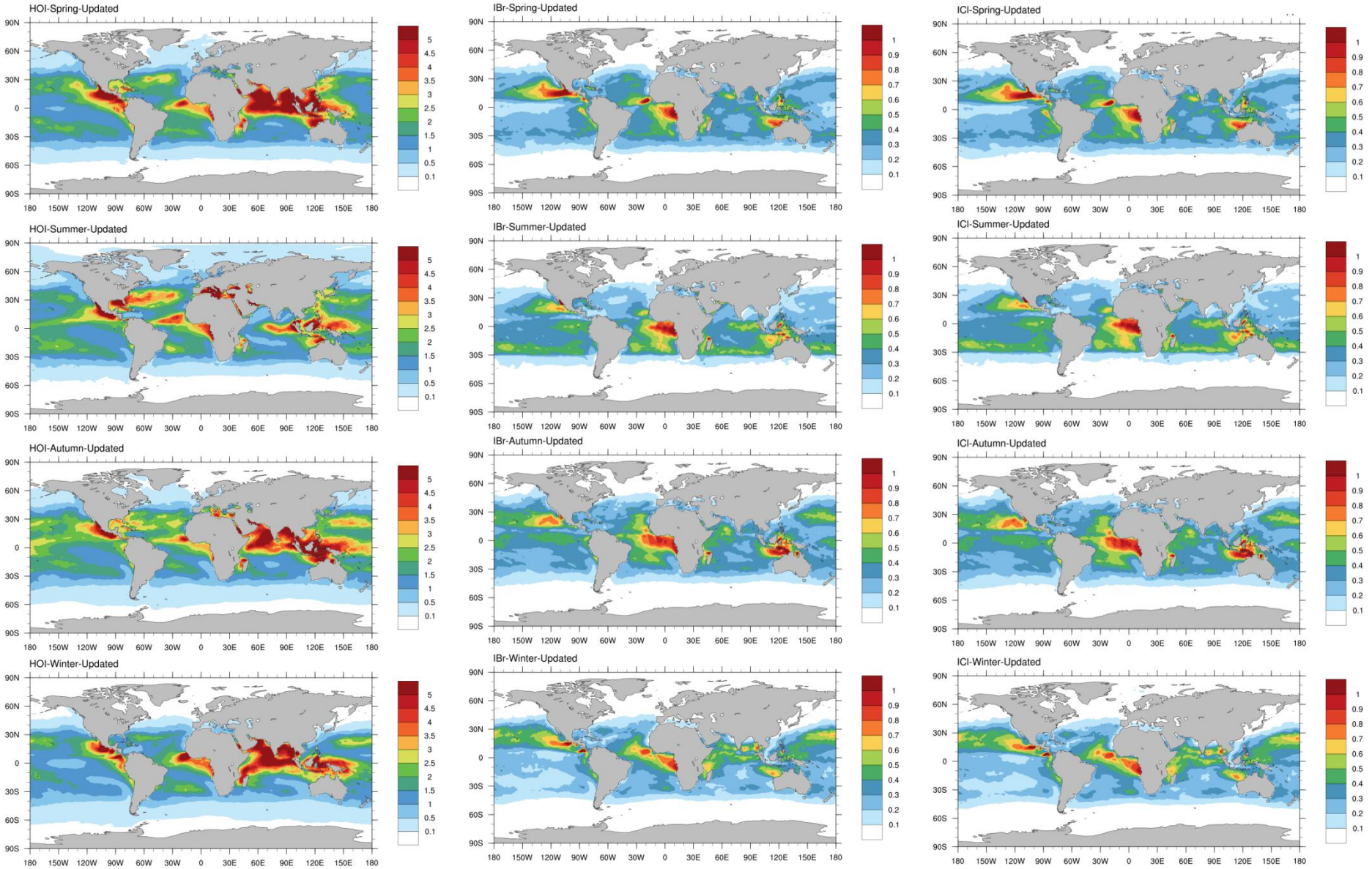

55 **Figure S6.** Simulated distribution of seasonal average mixing ratios (pptv) of HOI, IBr, and ICl in the MBL in the Updated case. Boreal seasons are used here. Spring includes March, April, and May; Summer includes June, July, and August; Autumn includes September, October, and November; Winter includes December, January, and February.

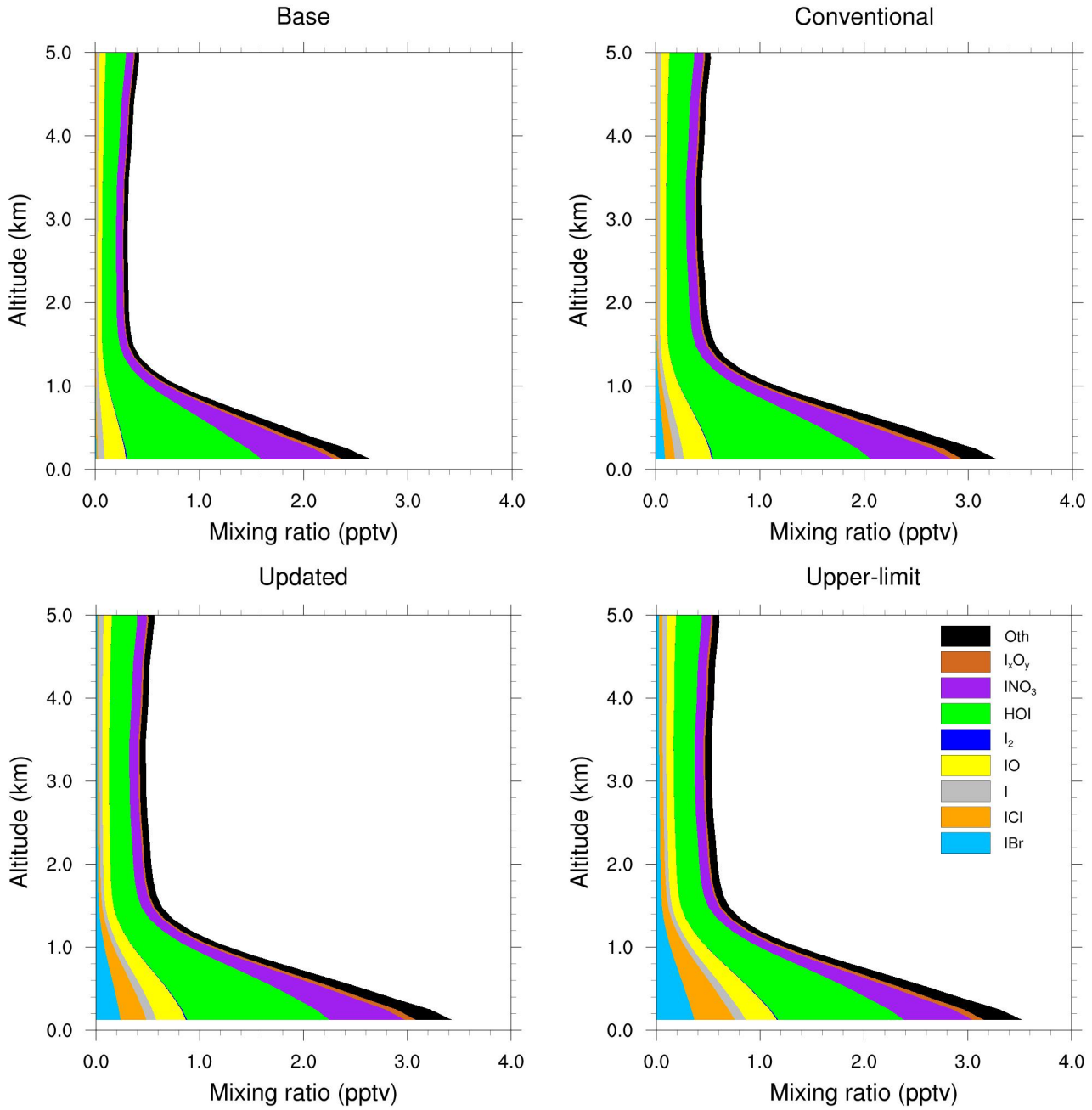

Figure S7. Vertical distribution of inorganic iodine species over the global ocean in the Base, Conventional, Updated, and Upper-limit scenarios. ”Oth” is the sum of other inorganic iodine species (OIO, HI, INO, and INO_2).

60

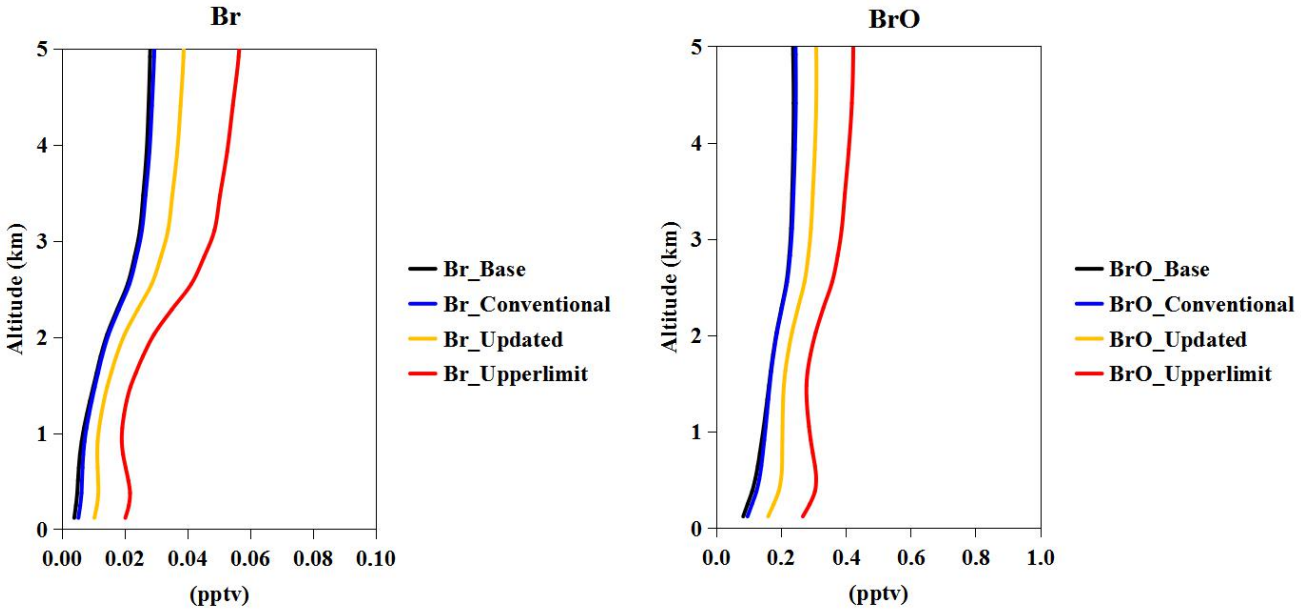

Figure **S8**. Vertical distribution of the mixing ratios of Br (pptv) and BrO (pptv) over the global ocean in the Base, Conventional, Updated, and Upper-limit scenarios.

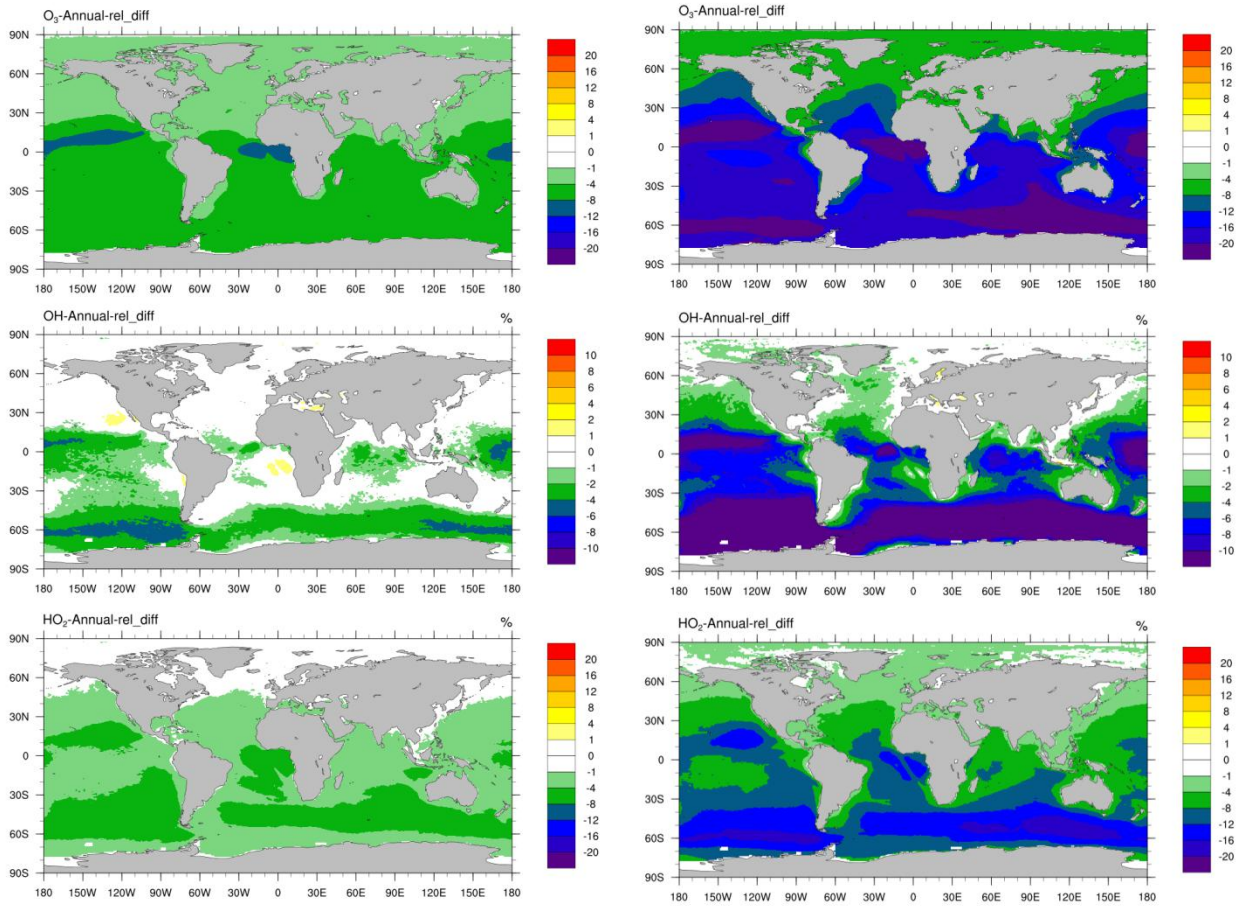

Figure S9. Simulated annual average of relative change (%) in O_3 (diurnal average), OH (sunlit time average), and HO_2 (sunlit time average) in the MBL between Base and Conventional cases (left) and between Base and Upper-limit case (right).

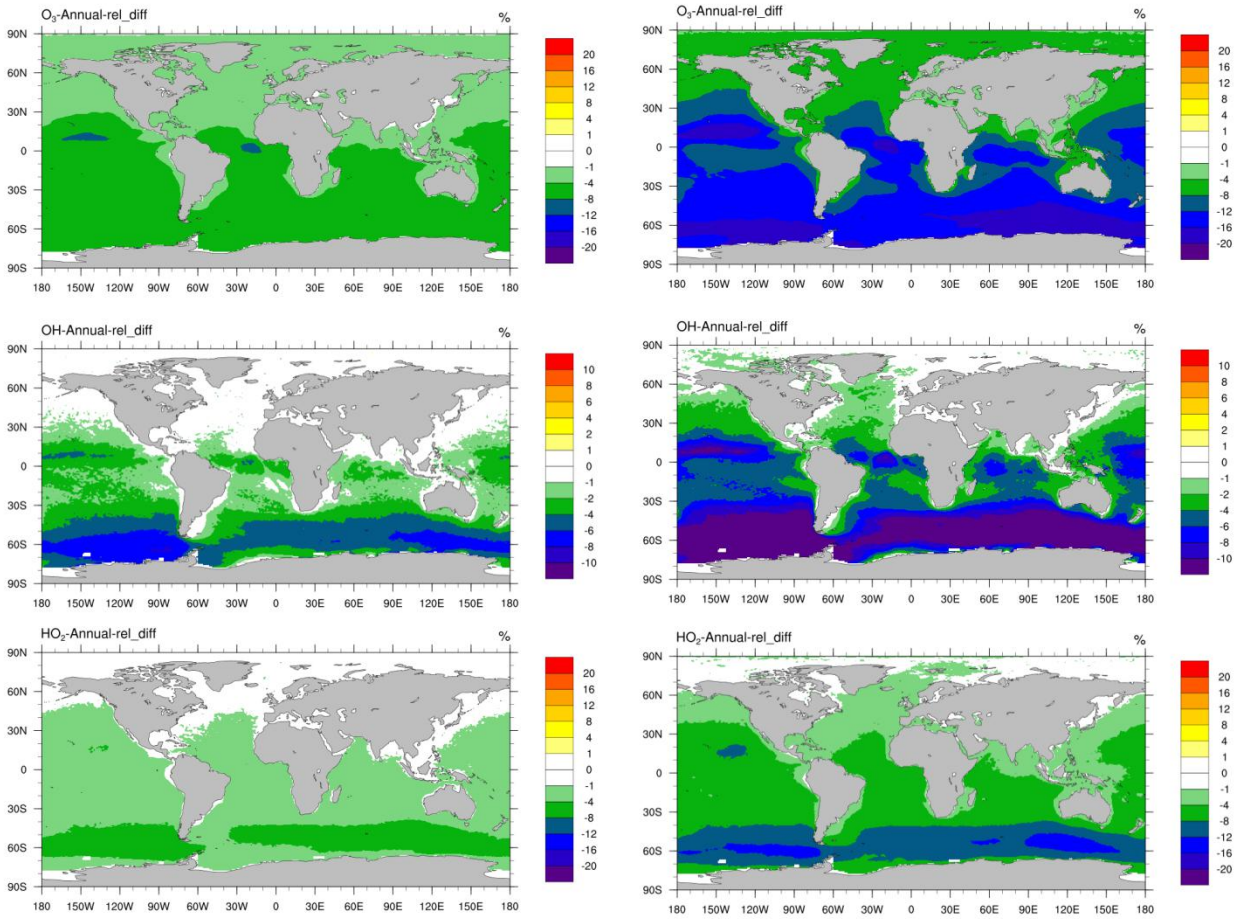

Figure S10. Simulated annual average of relative change (%) in O_3 (diurnal average), OH (sunlit time average), and HO_2 (sunlit time average) in the MBL between Conventional and Updated cases (left) and between Conventional and Upper-limit cases (right).

Reference

Archibald, A. T., J. L. Neu, Y. F. Elshorbany, O. R. Cooper, P. J. Young, H. Akiyoshi, R. A. Cox, et al. 2020. "Tropospheric Ozone Assessment Report." Elementa: Science of the Anthropocene 8 (1): 1–79. https://doi.org/10.1525/elementa.2020.034.

Dix, Barbara, Sunil Baidar, James F. Bresch, Samuel R. Hall, K. Sebastian Schmidt, Siyuan Wang, and Rainer Volkamer. 2013. "Detection of Iodine Monoxide in the Tropical Free Troposphere." Proceedings of the National Academy of Sciences of the United States of America 110 (6): 2035–40. https://doi.org/10.1073/pnas.1212386110.

Großmann, K., U. Frieß, E. Peters, F. Wittrock, J. Lampel, S. Yilmaz, J. Tschritter, et al. 2013. "Iodine Monoxide in the Western Pacific Marine Boundary Layer." Atmospheric Chemistry and Physics 13 (6): 3363–78. https://doi.org/10.5194/acp-13-3363-2013.

Mahajan, A. S., J. C. Gómez Martín, T. D. Hay, S. J. Royer, S. Yvon-Lewis, Y. Liu, L. Hu, et al. 2012. "Latitudinal Distribution of Reactive Iodine in the Eastern Pacific and Its Link to Open Ocean Sources." Atmospheric Chemistry and Physics 12 (23): 11609–17. https://doi.org/10.5194/acp-12-11609-2012.

Mahajan, A S, J. M.C. Plane, H Oetjen, L Mendes, R W Saunders, A. Saiz-Lopez, C E Jones, L. J. Carpenter, and G. B. McFiggans. 2010. "Measurement and Modelling of Tropospheric Reactive Halogen Species over the Tropical Atlantic Ocean." Atmospheric Chemistry and Physics 10 (10): 4611–24. https://doi.org/10.5194/acp-10-4611-2010.

Mahajan, Anoop S., Liselotte Tinel, Shrivardhan Hulswar, Carlos A. Cuevas, Shanshan Wang, Sachin Ghude, Ravidas K. Naik, et al. 2019a. "Observations of Iodine Oxide in the Indian Ocean Marine Boundary Layer: A Transect from the

Tropics to the High Latitudes." Atmospheric Environment: X 1 (January): 100016. https://doi.org/10.1016/j.aeaoa.2019.100016.

Mahajan, Anoop S., Liselotte Tinel, Amit Sarkar, Rosie Chance, Lucy J. Carpenter, Shrivardhan Hulswar, Prithviraj Mali, Satya Prakash, and P. N. Vinayachandran. 2019b. "Understanding Iodine Chemistry Over the Northern and Equatorial Indian Ocean." Journal of Geophysical Research: Atmospheres 124 (14): 8104–18. https://doi.org/10.1029/2018jd029063.

Martín, Juan C.Gómez, Anoop S. Mahajan, Timothy D. Hay, Cristina Prados-Román, Carlos Ordóñez, Samantha M. Macdonald, John M.C. Plane, et al. 2013. "Iodine Chemistry in the Eastern Pacific Marine Boundary Layer." Journal of Geophysical Research Atmospheres 118 (2): 887–904. https://doi.org/10.1002/jgrd.50132.

Prados-Roman, C., C. A. Cuevas, T. Hay, R. P. Fernandez, A. S. Mahajan, S. J. Royer, M. Galí, et al. 2015. "Iodine Oxide in the Global Marine Boundary Layer." Atmospheric Chemistry and Physics 15 (2): 583–93. https://doi.org/10.5194/acp-15-583-2015.

Read, Katie A., Anoop S. Mahajan, Lucy J. Carpenter, Mathew J. Evans, Bruno V.E. Faria, Dwayne E. Heard, James R. Hopkins, et al. 2008. "Extensive Halogen-Mediated Ozone Destruction over the Tropical Atlantic Ocean." Nature 453 (7199): 1232–35. https://doi.org/10.1038/nature07035.